WORLD CONFERENCE ON TIMBER ENGINEERING 2025
BRISBANE, AUSTRALIA
Advancing Timber for the Future Built Environment

Rotational performance of glulam pre-engineered beam-column joints

Zhichao Zheng[1], Xiaoyue Zhang[2]*, Weiguo Long[3], Yu Shi[4], Gang Xiong[5], Jiajia Ou[6], Zhigang Zhang[7]

ABSTRACT: Beam-column joints have been experimentally demonstrated to be critical yet vulneralble components of timber frame structures. A novel pre-engineered beam-hanger (PEBH) connection, mainly used for mass timber buildings, was proposed. To investigate the rotational performance of the connection, monotonic and cyclic tests were performed on four beam-column joints specimens. Experimental results show that stiffener effectively enhance the moment-resisting capacity and initial stiffness of the connection, but at the expense of reduced deformation capacity. Additionally, simplified numerical models were developed to simulate the hysteretic response of the conenction.

KEYWORDS: Glulam frame, Beam-column joint, Tests, Moment resistance, Initial stiffness

1 – INTRODUCTION

1.1 BEAM-HANGER CONNECTIONS

In recent years, there is increasing interest in using timber for modern construction due to its combination of aesthetics, structural performance, opportunity for innovation, constructability, and low carbon profile [1]. Beam-column structures allowed for buildings to be assembled quickly and cost-effectively, leding to the use of heavy timber structures for all types of building. However, the interruption of wood fibres at the intersections of beam-column joints presents a significant hurdle for the efficient transmission of moments between these structural elements. Unlike steel and concrete, which permit the creation of rigid portal joints through welding (steel) or the monolithic integration of the joint (concrete), the disruption in wood fibres at the junction of beams and columns, together with the low strength in the direction perpendicular to the fibres, makes the establishment of continuous connections for bending moments very challenging [2].

The bolted connection with slotted-in steel plate are commonly used in the modern glulam structures [4][5]. Research efforts have been made for many years to analyze the mechanical behaviors of such connections [3][8]. The extensivle test results showed that the moment resistance of glulam bolted connections was quite low, and unexpected brittle failure mode often occurred when the beam-column connections experienced large inter-story displacement [7][8].

Pre-engineered beam-hanger (PEBH) connection system are widely used in mass timber buildings for beam-column joints. These systems offer advantages over bolted or nailed connections because they can be pre-installed, allowing for easier and fast constructionby simply attaching the beam to its column member on site [9]-[11].

(a) CBH (b) Ricon S VS (c) Ricon Prototype (d) Megant

Fig.1 Common PEBH connections

Fig. 1 shows the common PEBH connections, typically designed as “shear” connectors to transfer loads from beams to columns. Therefore, these beam-hanger connections are assumed to be “pin-connections” and are

[1] Zhichao Zheng, School of Civil Engineering, Chongqing University, Chongqing, China, zhichaozheng1@163.com
[2]* Xiaoyue Zhang, School of Civil Engineering, Chongqing University, Chongqing, China, xiaoyuezhang@cqu.edu.cn
[3] Weiguo Long, China Southwest Architectural Design and Research Institute Corp. Ltd., Chengdu, China, xnymjg@cscec.com
[4] Yu Shi, School of Civil Engineering, Chongqing University, Chongqing, China, shiyucivil@cqu.edu.cn
[5] Gang Xiong, School of Civil Engineering, Chongqing University, Chongqing, China, 195704148qq.com
[6] Jiajia Ou, China Southwest Architectural Design and Research Institute Corp. Ltd., Chengdu, China, ouyangjia28@126.com
[7] Zhigang Zhang, School of Civil Engineering, Chongqing University, Chongqing, China, zhangzg@cqu.edu.cn

https://doi.org/10.52202/080513-0392

not intended to be part of the lateral-load resisting system of a building.

1.2 OBJECTVIES

At present, comprehensive research on the mechanical properties of PEBH connection remains limited, with most studies focusing on a small number of experiments conducted independently by manufacturers [12]-[15]. To address the current lack of research on PEBH connection, this paper proposes a new connection system. As shown in Fig. 2, the system is used when connecting two members together, for example in a beam-column joints or onther vertical connection. The novel connection system consists of two parts, one part screwed to the first member and the other to the second member. The members are then slotted together. The system is designed to resist tension, compression, and shear. The metal parts are fixed with threaded screws to the timber members. The system can also be used to attach timber members to steel members. This connection system has no visible parts in its final installation.

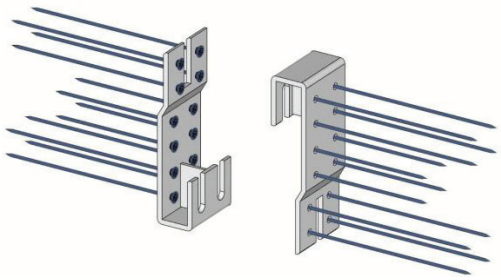

Fig. 2 Proposed PEBH connection system

2 – EXPERIMENAL TESTS

2.1 TEST SPECIMENS

Four beam-column joint specimens were tested, as listed in Table 1. The detailed geometrical dimension parameters of the connection are given in Fig. 3. The sizes of the beam and column members were 300 mm×150 mm×850 mm, 200 mm×225 mm×1000 mm, respectively..

Table 1: Tested specimens

Specimen	Stiffener	Loading protocol
CN-L-M	None	Monotonic
CN-L-C		Cyclic
CR-L-M	Stiffener	Monotonic
CR-L-C		Cyclic

2.2 MATERIALS

Glulam beams and columns used in this study graded as TCT36. The connectors were fabricated from Q235B steel. The self-tapping screws (STSs) used as fasteners in PEBH connection were of the product type KonstruX - HF with diameter of 8.0 mm, procured from Eurotec [16].

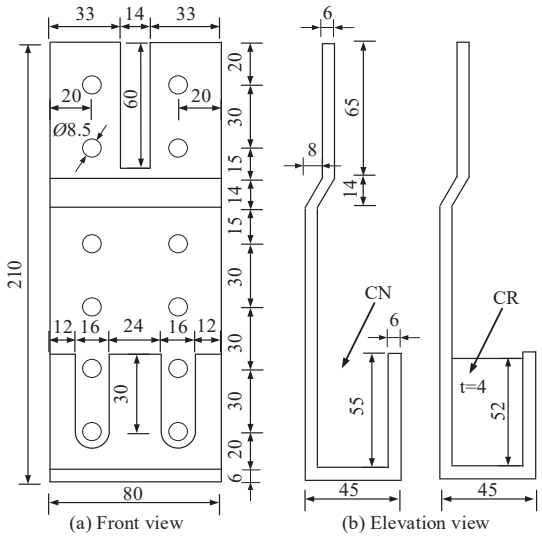

Fig. 3 Detail size of the PEBH connection (mm)

2.3 TEST SET-UP

All tests were conducted in the laboratory of Chongqing University, Congqimng, China. As shown in Fig. 4, the top end of the beam member was connected to a horizontal actuator through a hinge. The hydraulic actuator had a maximum loading capacity of 100 kN and a stroke range of 250 mm in both directions (push and pull). The load and displacement were defined as positive when the joints specimens were pushed to the right, while negative values were defined when the wall is pulled to the left. The glulam column members was horizontally placed accordingly the bottom of the speciemn was avoided to directly contact the steel baseplate in the ground [17]. The transtional displacemnts of the glulam column were limited by the combination of two steel beam and four anchor bolts.

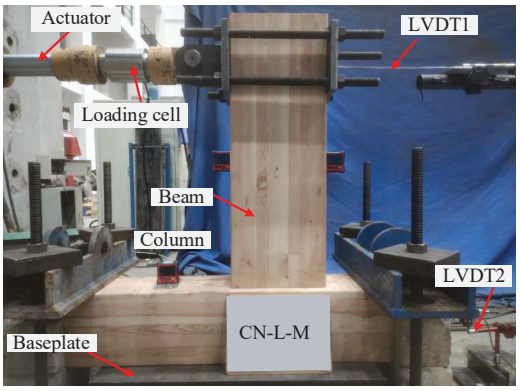

Fig. 4 Loading apparatus

As shown in Fig. 4, two linear variable displacement transducers (LVDTs) with 200 mm meauring range were distributed along the height of the beam to obtain the joint connection. LVDT1 was used tomonitor and record the horizontal displacment ($\Delta 1$) of the beam upper end. LVDT2 was placed at the column end to record the horizontal sliding ($\Delta 2$) of the entire specimen.

Test results demonstrated that the bending of the glulam beam and the rotation of the column can be ignored. Thus the moment M and joint rotation θ can be calculated according to Eq. (1) – (2).

$$M = F \times H \tag{1}$$

$$\theta = \arctan\left(\frac{\Delta_1 - \Delta_2}{H}\right)\frac{\pi}{180} \tag{2}$$

Where F is the horizontal force recorded by the loading cell, H (=710mm) is the vertical distance between the loading point and the lower end-face of the beam.

Both the monotonic and reversed cyclic loading tests were performend displacment-driven. For the monotonic loading tests, each specimen was loaded continuously at a constant rate of 5 mm/min until the applied load dropped to 80% of the maximum load according to ASTM D1761-88 [18].

In the reversed cyclic loading tests, the CUREE displacement-controlled cyclic protocol according to ASTM E2126-19 [19] was applied. As illustrated in Fig. 5, the CUREE protocol consisted of three different phases including initial cycles, primary cycles and trailing cycles. The protocol started with six initial cycles with an amplitude of 0.05Δ, followed by 14 initial cycles with an amplitude of 0.075Δ for the first seven cycles and an amplitude of 0.10Δ for the other seven cycles. The loading protocol had a primary cycle with an amplitude of 0.20Δ, followed by two trailing cycles with an amplitude of 75% of the primary cycle.

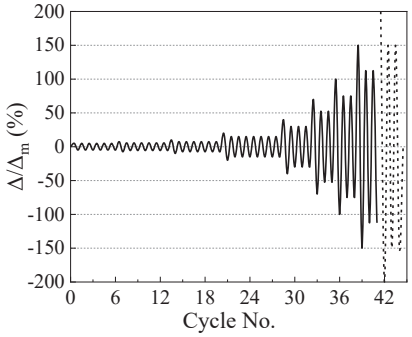

Fig. 5 CUREE protocol for cyclic tests

3 – EXPERIMENTAL RESULTS

3.1 FAILURE PATTERNS

Fig. 6 and 7 presents the failure patterns of the joint specimens under monotonic and cyclic loading, respectively.

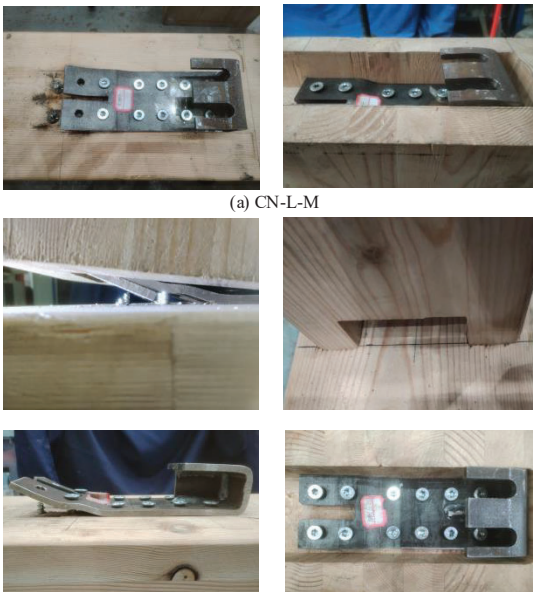
(a) CN-L-M

(b) CR-L-M

Fig. 6 Failure patterns of specimens loaded monotinically


(a) CN-L-C (b) CR-L-C

Fig. 7 Failure patterns of specimens loaded cyclically

During the initial loading stages, the specimens remained in an elastic state, and no noticeable deforamtion were observed on the surfaces of the glulam beams and columns. Since the connectors were concealed, deformations of both the connectors and the STSs were not visible. As the joint rotation further increased, the lower end of the beam began to show signs of separation from the column. For specimen CR-L-M, continuous

https://doi.org/10.52202/080513-0392

"hissing" sounds were heard, likely due to the tearing of the stiffener welds. Upon reaching the specimen's maximum moment, a distinct "bang" was heard as the two outermost STSs fractured almost simultaneously, leading to a sharp drop in the load-displacement curve.

As shown in Fig. 6, specimens CN-L-M and CR-L-M oucurred similar failure patterns. With increasing joint rotation, the column-end connector bent significantly, leading to the tensile rupture of the outermost row of screws. Apart from the pronounced compression deformation on the column surface at the beam-column interface caused by the compression of the beam end, the remaining portions of the glulam column and beam exhibited no obvious damage. Compared to CN-L-M, specimen CR-L-M exhibited smaller bending deformations at the cantilever and cleat zone due to the load distribution effect of the stiffener. However, the embedding deformation on the column surface of specimen CR-L-M was more pronounced than that of specimen CN-L-M.

The two beam-column joints under cyclic loading exhibited similar failure modes, as shown in Fig. 7. Specifically, tensile fracture occurred in the two outermost screws at the cantilever region of both the column-end and beam-end connectors, accompanied by noticeable bending deformation in the connectors at both ends.

3.2 MONOTONIC EXPERIMENTS

Fig. 8 shows the monotonic *M-θ* curves. It is notably that the stiffener significantly influence the moment – rotation response of the PEBH connection. Compared to bolted connections, the moment-rotation curve of the PEBH connection does not display a slip phase in the initial loading stage due to installation gaps, and the connection exhibits a higher initial rotational stiffness [8].

The *M-θ* curves can be categorized into three distinct phases: the initial linear-elastic phase, the plastic development phase, and a sharp descent after failure. After this descent, a gradual upward trend emerges, which can be attributed to the second row of screws taking over the primary load-bearing role following the failure of the outermost row of screws. Compared to specimen CR-L-M, the moment-rotation curve of specimen CN-L-M exhibits a longer plastic development phase, attributed to the lack of stiffener. This absence leads to more significant bending deformations in the column-end connector of specimen CN-L-M.

According to ASTM E2126 - 19 [20], the mechanical parameters of the tested specimens were determined using the equivalent energy elastic - plastic curve. Initial stiffness was calculated as the slope of the linear segment between 10% and 40% of the maxmum moment [21].

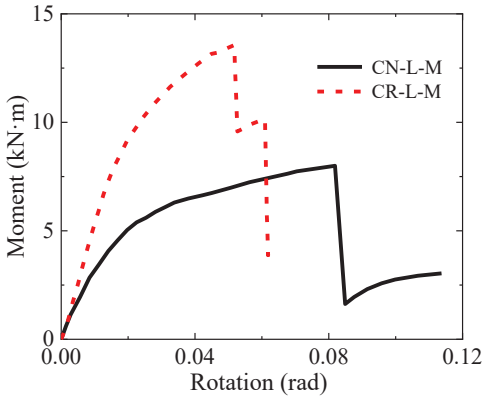

Fig. 8 Monotonic $M-\theta$ curves

Spciemn CR-L-M demonstrated a 76.3% increase in maximum moment and a 171.2% increase in initial stiffness compared to specimen CN-L-M, but its ductility decreased by 40.0%. However, the peak rotation of specimen CN-L-M at the maximum moment is 0.082, which is 58% higher than the 0.052 observed for specimen CR-L-M. This indicates that stiffener can effectively increase the maximum moment and rotational stiffness of the PEBH connection, but significantly reduce its deformability and ductility.

3.3 CYCLIC EXPERIMENTS

Fig. 9 shows the cyclic *M-θ* curves of the two specimens and envelope curves comparison. Please note that the hysterestic curves of the two specimens are in different scales in Fig. 9. It can be observed that the hysteresis curves of both specimens exhibit a pronounced pinching effect, similar to that of bolted connection.

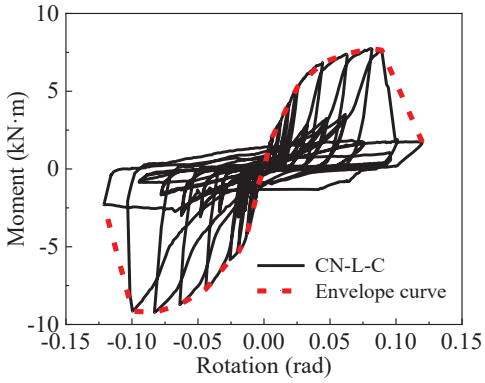

(a) CN-L-C

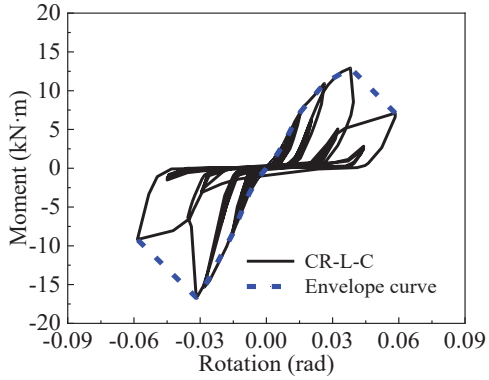

(a) CR-L-C

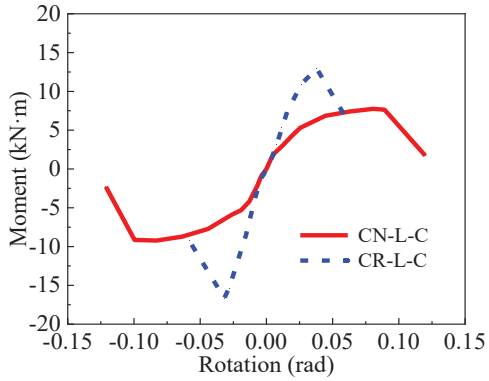

(c) Comparison of envelope curves

Fig. 9 Cyclic moment – rotation cresponse

Stiffness degradation

After the glulam embedment compression deformation and the bending deformation of steel connectors occurred, the rotational stiffness of the specimens declined gradually with the increased rotational displacement in the low frequency cyclic loading test. To display the phenomenon of stiffness degradation, the secant stiffness K_i (in units of kN·m/rad) of specimens is calculated by Eq. (3) [21].

$$K_i = \frac{|+M_i|+|-M_i|}{|+\theta_i|+|-\theta_i|} \tag{3}$$

Where K_i is the secant stiffness of the i-th primary cycle (kN·m) and is the rotation corresponding to the maximum moment of the i-th primary cycle (rad).

The rotational stiffness during cyclic loading for the two specimens is presented in Fig. 10. When the joint rotation is less than $0.2\Delta_c$, the stiffness of specimen CR-L-C is comparatively low, which may be attributed to manufacturing tolerances and installation gaps [22]. As the joint rotation increases, the plastic deformation of the connectors, screws, and glulam components also increases, leading to a gradual reduction in the rotational stiffness of the joint. Eventually, the beam-column joint with PEBH connection failed due to tensile fracture of the screws, resulting in a rapid decline in the rotational stiffness. It is evident that, throughout the entire reversed cyclic loading process, specimen CR-L-C exhibits significantly greater rotational stiffness than specimen CN-L-C

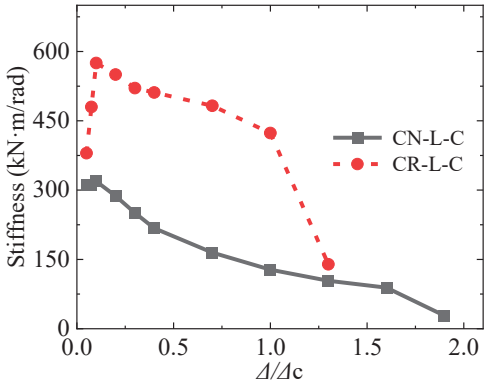

Fig. 10 Stiffness degradation of the specimens

Energy dissipation

The equivalent viscous damping ratio (EVDR), is used to quantify the energy dissipation capacity of the connections. The EVDR can be calculated by Eq. (4) [21][22].

$$\text{EVDR} = \frac{1}{2\pi}\frac{S_{\text{Loop}}}{S_{\Delta+}+S_{\Delta-}} \tag{4}$$

Where S_{Loop} is the area enveloped by each complete hysteretic loop. $S_{\Delta+}$ and $S_{\Delta-}$ represent the areas enclosed by two triangles, each having the same maximum moment and maximum rotation as the hysteresis loop during positive and negative loading of the PEBH connection.

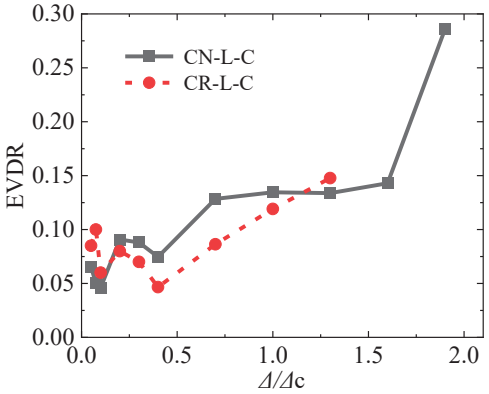

Fig. 11 EVDR

At the initial loading stage (Δ/Δ_c<0.4), the EVDR of both specimens are low (Fig. 11), illustrating that speimens perform elastic response. Subsequently, the EVDR of

https://doi.org/10.52202/080513-0392

specimen CR-L-C rapidly increases to joint failure, while the EVDR curve of specimen CN-L-M gradually rises over a longer period before suddenly increasing to joint failure. This behavior of specimen CN-L-C is similar to the longer plastic development phase observed in its skeleton curve.

4 – NUMERICAL SIMULATION

OpenSees [23] is a widely used and powerful software framework designed to simulate the nonlinear behavior of structural components and systems. Its versatility in modeling complex material properties, geometric configurations, and various loading conditions makes it a critical tool in earthquake engineering. In this study, OpenSees is employed to simulate the hysteretic response of the beam-column joints with PEBH connection, providing valuable insights into the nonlinear behavior of these essential connections under seismic loading. The outcomes of these simulations will form a robust foundation for subsequent seismic analyses, enabling more accurate predictions of structural performance during earthquakes and assisting in the optimization of seismic designs to enhance overall resilience.

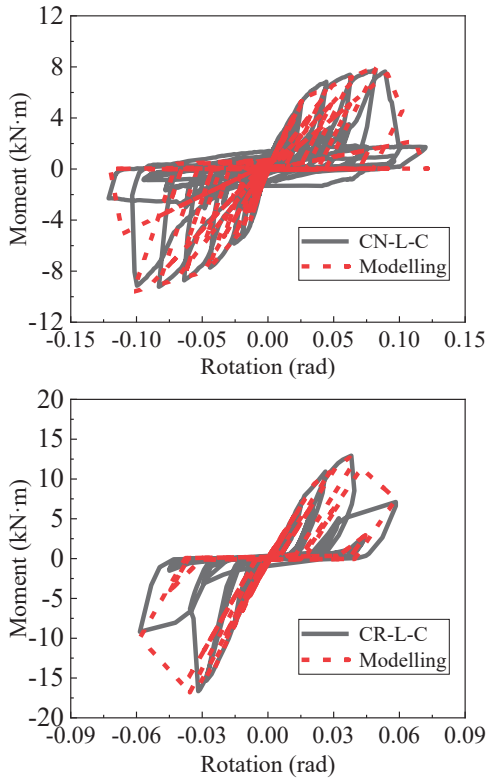

Fig. 14 Validation of the numerical model

Glulam beams and columns were modelled with elstic BeamColumn element. The twoNodeLink elements was applied to model the hysteretic response of the beam-column joint. It was described by using Pinching4 uniaxial material to reflect the pinched effect during cyclic loading [24]. Fig. 12 compares the hysterestic response from the cyclic loading and OpenSees. It was revealed that the simulated and measured M-θ curves showed a good agreement, and the mumerical model effectively predicted the initial stiffness of the spcimens.

5 – CONCLUSION

The rotational perforamnce of the newly proposed PEBH connection was studied experimentally and numerically. The experimental results indicate that the PEBH connection has a higher initial stiffness than the bolted connection. While the inclusion of stiffener effectively improves the moment capacity and initial stiffness of the connection, it also reduces its deformation capacity. In addition, simplified numerical models, developed by OpenSees, effectively predict the hysteretic response of the PEBH connection.

6 – ACKNOWLEDGEMENTS

The authors express their sincere gratitude for the financial support provided by the National Natural Science Foundation of China (No. 52478135); The National Key R&D Program of China (2021YFF0501004); The Chongqing Technology Innovation and Application Development Project (Grant No. CSTB2022TIAD-KPX0138); Chongqing Natural Science Foundation (Grant No. CSTB2024NSCQ-MSX0572); Open Research Fund for Key Laboratory of Building Structure Reinforcement and Underground Space Engineering, Ministry of Education (Grant No. MEKL202204); the Entrepreneurship and Innovation Support Program for Overseas-educated student in Chongqing China (Grant No. CX2021085).

6 – REFERENCES

[1] Ren G, Xue J, Ding Y. Effect of infilled CLT shear walls on the lateral performance of glued-laminated timber frames: Experimental and numerical analysis[J]. Structures, 2023, 50: 80-96.

[2] Ribeiro A B. Moment resistant joints for timber frames[D]. Universidade de Coimbra, 2024.

[3] Shu Z, Li Z, Yu X, et al. Rotational performance of glulam bolted joints: Experimental investigation and analytical approach[J]. Construction and Building Materials, 2019, 213: 675-695.

[4] Dorn M, de Borst K, Eberhardsteiner J. Experiments on dowel-type timber connections[J]. Engineering structures, 2013, 47: 67-80.

[5] Xu B H, Bouchaïr A, Taazount M, et al. Numerical and experimental analyses of multiple-dowel steel-to-timber joints in tension perpendicular to grain[J]. Engineering Structures, 2009, 31(10): 2357-2367.

[6] Zhang J, Liu D, Liu Z, et al. Rotational behavior of bolted post-to-beam glulam connections with friction damped knee brace[J]. Journal of Building Engineering, 2023, 76: 107215.

[7] Lam F, Gehloff M, Closen M. Moment-resisting bolted timber connections[J]. Proceedings of the Institution of Civil Engineers-Structures and Buildings, 2010, 163(4): 267-274.

[8] He M, Liu H. Comparison of glulam post-to-beam connections reinforced by two different dowel-type fasteners[J]. Construction and Building Materials, 2015, 99: 99-108.

[9] Vojtilaa G, MacDougallb C. Seismic performance of timber connections for sustainable tallwood building[J]. Scientific Committee, 19.

[10] Leach H. Interstorey drift performance of timber beam-hanger connections[D]. Queen's University, Kingson, Ontario, Canada, 2018. Master of degree.

[11] Engström T. Structural Connections in Modern Timber Construction[J]. 2024.

[12] https://mtcsolutions.com/projects/first-tech-federal-credit-union/.

[13] https://ssttoolbox.widen.net/view/pdf/wwzoznjs88/LSCBHDRIFT23.pdf?t.download=true&u=cjmyin.

[14] MTC solution, Inc. Inter-Story Drift Testing of KNAPP RICON S VS Connectors[EB/OL]. [2017-06-09]. https://mtcsolutions.com/wp-content/uploads/2017/06/Inter-Story-Drift-Performance-of-Concealed-Connection-Systems-2017_Disclaimer-Update.pdf

[15] Vojtila G. Cyclic Testing of Pre-Engineered Beam-Hanger Connections & Reinforcement of Holes in Glulam Beams Using Self-Tapping Screws[D]. Queen's University (Canada), 2020.

[16] https://www.eurotec.team/en/products/timber-engineering/konstrux-fully-threaded-screw.

[17] Fang L, Qu W, Zhang S. Rotational behavior of glulam moment-resisting connections with long self-tapping screws[J]. Construction and Building Materials, 2022, 324: 126604.

[18] American Society for Testing and Materials (ASTM), ‘‘Standard test methods for mechanical fasteners in wood”, ASTM D1761–88, West Conshohocken, PA, 2000.

[19] E2126-19 Standard Test Methods for Cyclic (Reversed) Load Test for Shear Resistance of Vertical Elements of the Lateral Force Resisting Systems for Buildings, American Society for Testing and Material Standards (ASTM), West Conshohocken, USA, 2019.

[20] E2126-19 Standard Test Methods for Cyclic (Reversed) Load Test for Shear Resistance of Vertical Elements of the Lateral Force Resisting Systems for Buildings, American Society for Testing and Material Standards (ASTM), West Conshohocken, USA, 2019.

[21] He M, Luo J, Tao D, et al. Rotational behavior of bolted glulam beam-to-column connections with knee brace[J]. Engineering Structures, 2020, 207: 110251.

[22] Xie Q, Liu Y, Zhang B, et al. Seismic performance of glulam frame with friction damper and column shoe: Experimental investigation and simplified numerical model[J]. Engineering Structures, 2024, 298: 117036.

[23] McKenna F, Fenves G, Scott M, Jeremic B. Open system for earthquake engineering simulation (OpenSees). Rep. Prepared for the Pacific Earthquake Engineering Research Center. Berkeley, CA: College of Engineering, Univ. of California; 2000.

[24] Ren X C, Meng Z B, Wu Y J, et al. Seismic performance of traditional Chinese timber structure: A Case of Guangyue tower[J]. Journal of Building Engineering, 2025, 100: 111690.

https://doi.org/10.52202/080513-0392